J Polym Res (2011) 18:401–408
DOI 10.1007/s10965-010-9430-4

ORIGINAL PAPER

Effects of modified vermiculite on the synthesis and swelling behaviors of hydroxyethyl cellulose-*g*-poly(acrylic acid)/vermiculite superabsorbent nanocomposites

Jinlei Wang · Wenbo Wang · Yian Zheng · Aiqin Wang

Received: 13 December 2009 / Accepted: 25 March 2010 / Published online: 7 April 2010

Abstract A series of hydroxyethyl cellulose-*g*-poly(acrylic acid)/vermiculite (HEC-*g*-PAA/VMT) superabsorbent nanocomposites were prepared by radical solution polymerization among hydroxyethyl cellulose (HEC), partially neutralized acrylic acid (AA), raw vermiculite (RVMT), acidified vermiculite (AVMT) and organo-vermiculite (OVMT) in the presence of initiator ammonium persulfate (APS) and crosslinker *N,N'*-methylenebisacrylamide (MBA). FTIR results revealed that AA was grafted onto HEC backbone and VMT participated in polymerization. VMT was exfoliated during polymerization reaction and a nanocomposite structure was formed as shown by XRD and TEM analysis. Effects of VMT content, concentration of HCl solution and organification degree of OVMT on water absorbency were investigated and the swelling kinetics of the developed nanocomposites was also evaluated. Results showed that incorporation of VMT greatly enhanced the water absorbency, and the modified VMT by acidification and organification can improve the water absorbency more remarkably than raw one. OVMT can improve the swelling capabilities and swelling rate to the highest degree in contrast to RVMT and AVMT.

Keywords Hydroxyethyl cellulose · Vermiculite · Superabsorbent nanocomposites · Graft copolymerization · Swelling

J. Wang · W. Wang · Y. Zheng · A. Wang (✉)
Center of Eco-material and Green Chemistry, Lanzhou Institute of Chemical Physics, Chinese Academy of Sciences, Lanzhou 730000, People's Republic of China
e-mail: aqwang@licp.cas.cn

J. Wang · W. Wang
Graduate University of the Chinese Academy of Sciences, Beijing 100049, People's Republic of China

Introduction

Superabsorbents are slightly crosslinked 3-D hydrophilic polymer networks which can highly swell but do not dissolve in aqueous media. Comparing with general absorbents (e.g. cotton, sponge, towel, and colloid silicate, etc.), superabsorbents can absorb and retain large volumes of aqueous fluids even under certain heating or pressure. By right of this, superabsorbents have attracted continuous interests and found potential applications in many fields, such as personal hygiene products [1], controlled release carrier of drug [2], coal dewatering [3], agriculture [4–6] and wastewater treatment [7, 8], etc. With the increasing resource and environment issues, polysaccharides-based materials have received extensive attention because their unique renewable, nontoxic, biodegradable and biocompatible characteristics [9, 10]. Many polysaccharides including starch [11, 12], cellulose [13, 14], sodium alginate [15], chitosan [16, 17], guar gum [18], carrageenan [19], gelatin [20], and tragacanth gum [21] have been focused as a matrix for the preparation of environmentally friendly superabsorbents. Among them, cellulose and its derivatives showed unique advantages because they are the most abundant natural polysaccharide with low cost and better biodegradability and biocompatibility. Hydroxyethyl cellulose (HEC) is a representative cellulose derivative with excellent water solubility and biocompatibility [22]. The unique properties of HEC allow it to be used in many biotechnological, biophysical and industrial fields. Due to the abundant reactive −OH groups on the HEC chains, HEC can be easily modified by grafting polymerization with hydrophilic vinyl monomers to derive new materials with improved properties.

Recently, organo-inorganic superabsorbent composites derived from the modification of organic polymer by

inorganic clays have attracted great attention because such materials frequently showed low production cost and improved performance [23, 24]. Vermiculite (VMT) is a trioctahedral 2:1 layered silicate similar in texture to mica, and it is abundant and much cheaper in comparison with montmorillonite, hetorite, and saponite [25]. The properties of traditional superabsorbent can be greatly improved by introducing RVMT into its network structure [26]. It is desired that the modification of RVMT by some facile methods can further improve the comprehensive performance of superabsorbent. Acid activation and organification modification are the preferred methods employed to improve the surface properties of clay minerals. Appropriate acid treatment can improve the activity of surface Si–OH groups of clays by the removal of carbonate impurities and organic materials as well as the disaggregation of clay congeries [27]. Organification modification of layer silicate with cationic surfactant alters the surface property and interlayer gap of clay minerals [28]. Thus, the physical and chemical properties of RVMT can be changed by the simple modification of acidification and organification.

As part of efforts to develop new kinds of natural polymer-based superabsorbents, the novel nanocomposites were prepared by radical solution polymerization using biodegradable hydroxyethyl cellulose (HEC) as polymeric matrix, acidified vermiculite (AVMT) and organo-vermiculite (OVMT) as the inorganic components. The structures of the developed nanocomposites were characterized by Fourier Transform Infrared (FTIR) spectroscopy, X-ray Diffraction (XRD) and transmission electron microscopy (TEM) analysis. In addition, the effects of VMT content, HCl concentration and organification degree of OVMT on the swelling properties were investigated systematically.

Experimental

Materials

Hydroxyethyl cellulose (HEC, practical grade, viscosity 4000 cP) was obtained from Serva Feinbiochemica (Heidelberg, Germany). Acrylic acid (AA, Chemically Pure, Shanghai Shanpu Chemical Factory, Shanghai, China) was distilled under reduced pressure before use. Unexpanded vermiculite (VMT) micropowder (Linze Colloidal Co., Gansu, China) was milled and passed through a 320-mesh screen prior to use. Ammonium persulfate (APS, analytical grade, Xi'an Chemical Reagent Factory, Xi'an, China) was recrystallized from water. *N,N'*-methylenebisacrylamide (MBA, Chemically Pure, Shanghai Chemical Reagent Corp., Shanghai, China) and cetyltrimethylammonium bromide (CTAB, Beijing Chemical Reagents Company, China) was used as purchased. Other reagents used were of analytical grade and all solutions were prepared with distilled water.

Acid activation of RVMT

RVMT powder (10.0 g) was dispersed in 100 mL HCl aqueous solution with the concentrations of 2 mol/L, 4 mol/L, 6 mol/L, 8 mol/L and 12 mol/L, and then the dispersion was vigorously stirred at room temperature for 2 h. The resultant acidified VMT (AVMT) product was isolated by centrifugation and washed with distilled water for several times to remove residual acid and other impurities until the pH value of washed solution reached 6. The final product was dried to constant weight in an oven at 70°C and passed through a 320-mesh sieve prior to use.

Organification modification of RVMT

Five different amounts of CTAB were dissolved in 100 mL distilled water, respectively. Then, 10.0 g RVMT was charged to the solution and followed by a vigorous stirring at room temperature for 4 h. The generated organo-vermiculite (OVMT) was isolated by suction filtration and fully washed with distilled water to remove residual CTAB until no Br^- can be detected by $AgNO_3$ solution (0.1 mol/L) from the filtrate. The final OVMT was dried to constant weight at 70°C and passed through a 320-mesh sieve.

The organification degree of OVMT (denotes the weight percent of organic cation in OVMT sample) was determined by thermogravimetric analysis: the dry OVMT sample (0.50 g) modified by different amount of CTAB and RVMT sample (0.50 g) was placed in the crucible after being accurately weighed, respectively. Then, the crucible was calcined in air at 800°C for 6 h. After reaching a constant weight, the samples were transferred to a desiccator and cooled to room temperature. Finally, these samples were weighed and the organification degree of OVMT was calculated according to Eqs. 1 and 2.

$$OD = (\Delta m_{\mathrm{OVMT}} - \Delta m_{\mathrm{RVMT}})/m_1 \times 100\% \quad (1)$$

$$\Delta m_{\mathrm{OVMT}} \text{ or } \Delta m_{\mathrm{RVMT}} = m_1 - m_2 \quad (2)$$

where OD is the organification degree of OVMT; Δm_{OVMT} and Δm_{RVMT} are the weight loss of OVMT and RVMT, respectively; m_1 and m_2 are the weight of the samples before and after calcining, respectively.. The dosage of CTAB and corresponding organification degree of OVMT was corresponded as follows (Dosage of CTAB/Organification degree):

0.3132 g/2.06 wt%; 0.6263 g/2.62 wt%; 1.2526 g/4.03 wt%; 2.5052 g/9.01 wt%; 3.7578 g/12.16 wt%.

Preparation of HEC-*g*-PAA/VMT superabsorbent nanocomposites

HEC (1.2 g) was dissolved in 32.6 mL distilled water in a 250-mL four-necked flask equipped with a mechanical stirrer, a reflux condenser, a nitrogen line and a thermometer. The solution was heated to 60°C and purged with N_2 for 30 min to remove the dissolved oxygen. Then, 3 mL of aqueous solution of initiator APS (72.0 mg) was added and stirred for 10 min. After cooling the reactants to 40°C, the mixed solution containing AA (7.2 g, neutralized with 8.2 mL 8.0 mol/L NaOH solution), crosslinker MBA (14.4 mg) and VMT powders (0.94 g) was added, and the temperature was slowly risen to 70°C and maintained for 3 h to complete the polymerization. The obtained gels were dried to constant weight at 70°C, and the dried gels were ground and passed through 40 to 80 mesh sieve (180~380 μm). HEC-*g*-PAA superabsorbent was prepared according to a similar procedure except without addition of VMT.

Measurements of equilibrium water absorbency and swelling kinetics

0.05 g sample was immersed in excess of aqueous solutions at room temperature for 4 h to reach swelling equilibrium. The swollen gels were then filtered using a 100-mesh screen. After weighing the swollen samples, the equilibrium water absorbency (Q_{eq}, g/g) of the superabsorbent was calculated using the following equation (Eq. 3):

$$Q_{eq} = (w_s - w_d)/w_d \tag{3}$$

where w_d and w_s are the weights of the dry sample and the swollen sample, respectively. Q_{eq} was calculated as grams of water per gram of sample.

Swelling kinetics of the superabsorbent was measured as follows: an accurate amount of sample (0.05 g) was poured into 400 mL distilled water. At certain time intervals, the water absorbency of the sample at a given time (Q_t, g/g) was measured by weighing the swollen gel and calculated according to Eq. 3. In all cases three parallel samples were used and the averages were reported in this paper.

Network parameter *M*c

The swelling properties of the hydrogel is dependent on the crosslinking density, which can be reflected by the average molar mass among the crosslinks, *M*c. *M*c value is reversibly proportional to crosslinking density and can be calculated by a previously developed method [29]. Typically, *M*c can be expressed as following equation (Eq. 4) according to Flory-Huggins theory [30]:

$$Mc = Q^{5/3} D_2 V_1 / (0.5 - X_1) \tag{4}$$

where Q represents the swelling capability of the hydrogel; D_2 denotes the density of hydrogel; V_1 denotes the molar volume of the solvent used for swelling studies and X_1 is the Flory-Huggins interaction parameter between solvent and hydrogel. Because it is difficult to determine X_1 by experiment, the linear relationship between X_1 and C (the volume fractions of methanol in methanol/water mixture) was established to determine X_1 value (Eq. 5).

$$X_1 = K_1 C + K_2 \tag{5}$$

After simplified above equations, it was concluded that the relations among each parameter follows Eq. 6.

$$D_2 V_1 Q^{5/3}{}_{\text{methanol-water}} = Mc(0.5 - K_1 C) \tag{6}$$

The plots of $D_2 V_1 Q_{\text{methanol-water}}{}^{5/3}$ against C give straight line, and the *M*c can be calculated according to the slope of the resulting line.

Characterizations

FTIR spectra were recorded on a Nicolet NEXUS FTIR spectrometer in 4,000−400 cm^{-1} region using KBr platelets. XRD analyses were performed using an X-ray power diffractometer with Cu anode (PAN analytical Co. X'pert PRO), running at 40 kV and 30 mA, scanning from 3° to 10° at 3°/min. TEM was performed on an instrument of JEM1200EX (Japan), and the powdered specimen was placed on the copper grids after sonicating its suspension in ethanol dried for 30 min.

Results and discussion

FTIR spectra

The FTIR spectra of RVMT, modified VMT and the corresponding nanocomposites with 10 wt% VMT are shown in Fig. 1. Compared with the spectra of RVMT (Fig. 1a), the absorption bands of AVMT at 1,419 cm^{-1} and 878 cm^{-1} (stretching and bending vibration of $CO_3{}^{2-}$ groups, respectively) disappeared, and the absorption band at about 3,422 cm^{-1} (stretching vibration of O–H groups) increased, indicating that carbonate impurities were removed from RVMT and the −OH group of VMT increased after acid-activated treatment [25]. It can be noticed from Fig. 1c that a batch of new bands at 2,918 cm^{-1}, 2,850 cm^{-1} and 1,472 cm^{-1} (asymmetrical stretching vibration, symmetrical stretching vibration and

bending vibration of $-CH_3$ and $-CH_2$ groups, respectively) appeared in the spectrum of OVMT. This result indicates that organic cations of CTAB have exchanged with the interlayer exchangeable cations of RVMT.

From Fig. 1d–h, it can be seen that the absorption band of HEC at 1,466 cm^{-1} (bending vibration of C–OH) disappeared and the new bands at 1,577 cm^{-1}, 1,455 cm^{-1} and 1,409 cm^{-1} (asymmetric and symmetric stretching vibration of $-COO^-$ groups, respectively) appeared in the spectra of HEC-*g*-PAA, HEC-*g*-PAA/RVMT, HEC-*g*-PAA/AVMT and HEC-*g*-PAA/OVMT after reaction (Fig. 1e–h). This observation reveals that poly(acrylic acid) chains had been grated onto HEC backbone. The absorption bands of VMT at 3,673 cm^{-1} and 1,636 cm^{-1} (stretching and bending vibration of (Si)O–H, respectively) almost disappeared after reaction (Fig. 1f–h). Also, the absorption band of VMT at 1,001 cm^{-1} (asymmetric stretching vibration of Si–O(H) groups) shifted to around 1,018 cm^{-1} and was obviously weakened in the spectra of HEC-*g*-PAA/RVMT, HEC-*g*-PAA/AVMT, and HEC-*g*-PAA/OVMT (Fig. 1f–h). This information indicates that VMT also participated in the graft copolymerization reaction through its active Si–OH groups [26, 31].

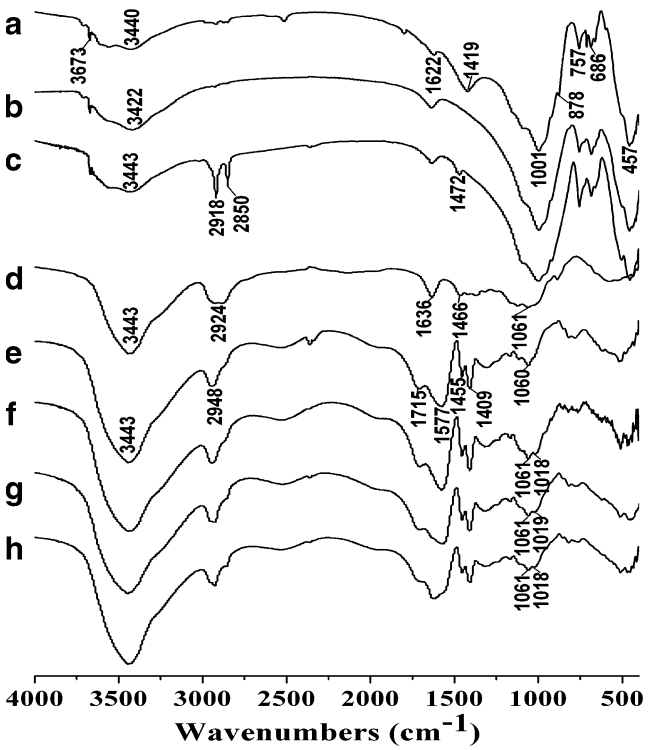

Fig. 1 FTIR spectra of **a** RVMT, **b** AVMT (C_{HCl}=2 mol/L), **c** OVMT (OD=2.62 wt%), **d** HEC, **e** HEC-*g*-PAA, **f** HEC-*g*-PAA/RVMT (10 wt%), **g** HEC-*g*-PAA/AVMT (C_{HCl}=2 mol/L; Content, 10 wt%), and **h** HEC-*g*-PAA/OVMT (OD=2.62 wt%; Content, 10 wt%)

XRD analysis

XRD patterns of RVMT, AVMT, OVMT, HEC-*g*-PAA/RVMT, HEC-*g*-PAA/AVMT and HEC-*g*-PAA/OVMT are shown in Fig. 2. RVMT showed reflections at 2θ=7.17°, 8.79°, and 9.78° (Fig. 2a). The diffraction peak at 2θ=7.17° (001, d=1.23 nm) represented the interlayer spacing of RVMT sample, while the peaks at 8.79° and 9.78° are due to the associated minerals in VMT [32]. After being treated with 2 mol/L HCl solution, the characteristic peak of RVMT at 2θ=7.17° (d=1.23 nm) shifted to 2θ=7.38° (d=1.20 nm) with weakened intensity and the diffraction peak at 2θ=8.79° shifted to 2θ=8.72° with remarkably increased intensity (Fig. 2b). The diffraction peak at 2θ=8.72° shows the existence of palygorskite [33]. These changes indicate that VMT may dissolve partially but the associated minerals were enriched during acidification [25]. After organification, a remarkable shift of the (001) diffraction peak from 2θ=7.17° (d=1.23 nm) to 2θ=5.06° (d=1.75 nm) was observed (Fig. 2c), suggesting that the alkyl chains of CTA^+ intercalated into the layer gallery of VMT and the interlayer spacing of VMT was expanded.

After polymerizing with HEC and AA, the characteristic (001) diffraction peak of VMT disappeared in the XRD patterns of HEC-*g*-PAA/RVMT, HEC-*g*-PAA/AVMT and HEC-*g*-PAA/OVMT (Fig. 2d–f). As is well known, the changes in interlayer spacing of layered silicates derived from (001) diffraction peak analysis is the criterion to identify the intercalated or exfoliated structure of nanocomposite [34]. Thus, the disappearance of (001) diffraction peaks of superabsorbent composites

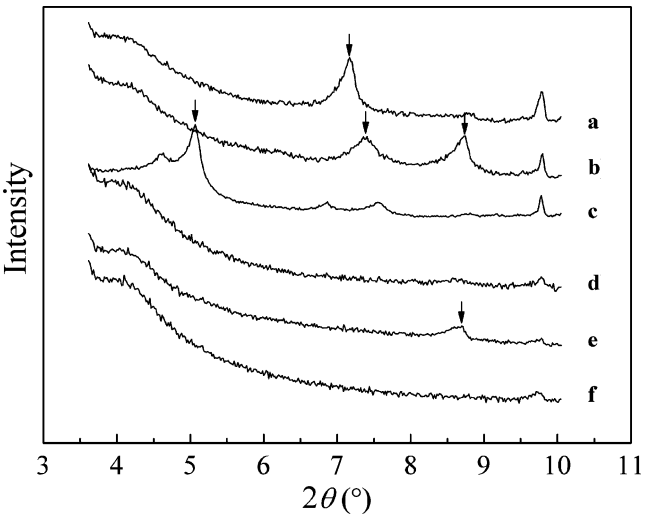

Fig. 2 XRD patterns of **a** RVMT, **b** AVMT (C_{HCl}=2 mol/L), (c) OVMT (OD=2.62 wt%), **d** HEC-*g*-PAA/RVMT (10 wt%), **e** HEC-*g*-PAA/AVMT (C_{HCl}=2 mol/L; Content, 10 wt%), and **f** HEC-*g*-PAA/OVMT (OD=2.62 wt%; Content, 10 wt%)

demonstrates that the modified VMT was exfoliated and dispersed in the polymer matrix at a nano-scale level and formed a nanocomposite structure [25].

TEM analysis

TEM images of HEC-*g*-PAA/AVMT and HEC-*g*-PAA/OVMT superabsorbent nanocomposites were observed and shown in Fig. 3. The exfoliated VMT platelets can be clearly observed in the TEM images of the nanocomposites, which indicate that VMT was exfoliated during polymerization and the exfoliated platelets led to a better dispersion in polymeric matrix without flocculation. This observation is accordant with the XRD results.

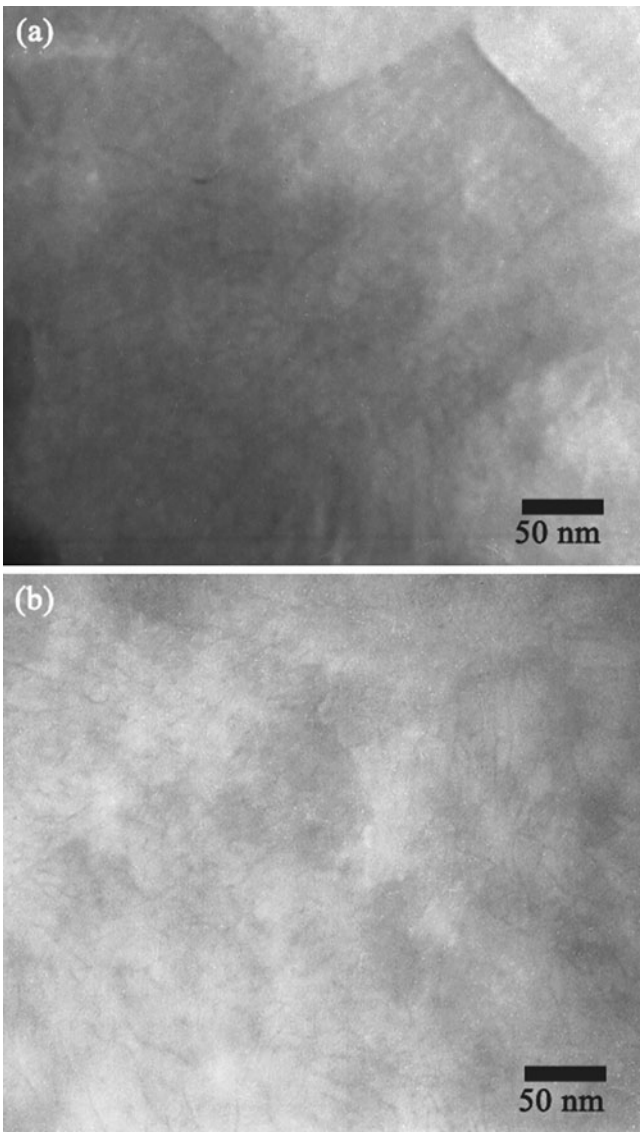

Fig. 3 TEM micrographs of HEC-*g*-PAA/AVMT (**a**) and HEC-*g*-PAA/OVMT (**b**) superabsorbent nanocomposites

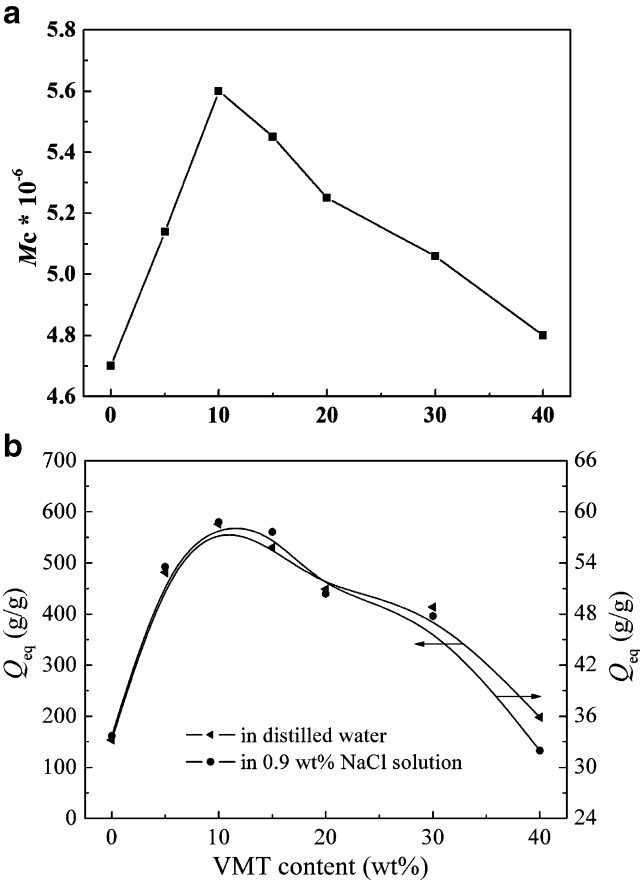

Fig. 4 Effects of VMT content on *M*c (**a**) and water absorbency (**b**) of HEC-*g*-PAA/VMT

Effects of VMT content on *M*c and water absorbency

As can be seen from Fig. 4, both the *M*c and water absorbency of the nanocomposite remarkably increased with the VMT content increasing to 10 wt% and then decreased with the further increase of VMT content. The same change trend for *M*c and water absorbency indicated that the swelling capability of the nanocomposite is mainly dependent on the crosslinking density of gel network. Compared with the VMT-free sample, the water absorption of the composite containing 10 wt% VMT increased by 263%. The great improvement of the water absorbency can be attributed to the following reason: the incorporation of rigid VMT platelets relieves the physical intertwisting of the grafted polymer chains and weaken the hydrogen-bonding interaction among hydrophilic groups. This contributes to decrease the physical crosslinking degree of hydrophilic network and improve the water absorbency. Thus, the water absorbency can be enhanced by introducing moderate amount of VMT.

However, an excessive addition of VMT (>10 wt%) leads to a reduction of water absorbency. This is because that the excess of VMT is physically filled in the network

space. On one hand, the ratio of hydrophilic groups in unit volume and the hydrophilicity of nanocomposite were decreased; on the other hand, the network voids for holding water was plugged up due to the physical stack of VMT in polymeric network. This results in the rapid reduction of water absorbency. But, it is worth pointing out that the water absorbency of the superabsorbent nanocomposite incorporating 40 wt% of VMT is still as much as that of VMT-free sample, which is favorable to reduce the production cost. The similar tendency can also be observed in poly (sodium acrylate)/vermiculite superabsorbent composite [26].

Effects of HCl concentration on water absorbency

As showed in Fig. 5, the water absorbency of HEC-*g*-PAA/AVMT was greatly improved after modified RVMT by 2 mol/L HCl, and was decreased with the further increase in HCl concentration. As mentioned above, acidification treatment can remove carbonate impurities and decompose the mineral congeries, which would expose the Si–OH groups and improve the activity of the Si–OH groups. In addition, the breakage of Si–O–Si bonds under the action of acid may form new silanol groups (see FTIR results) and balance their residual charge by accepting either proton or hydroxyl groups to form Si–OH groups [23, 35]. This contributes to enhance the activity of VMT, and is responsible for the enhancement of water absorbency. However, more H^+ would exchange the cations on the surface of VMT and more active surface Si–OH groups would be transformed into $Si–OH_2^+$ groups as increasing HCl concentration (>2 mol/L), and the crystalline structure of VMT would be destroyed at higher HCl concentration [36]. As a result, the amount of active sites on the VMT surface would be reduced and the polymeric networks would not form effectively, thus the water absorbency decreased.

Effect of organification degree of VMT on water absorbency

Alkylammonium ion exchange of layered silicate is the most common and effective modification method to prepare polymer/layered silicate nanocomposites [37]. As can be seen from Fig. 6, the water absorbency of HEC-*g*-PAA/OVMT nanocomposite increased with the increase of organification degree, reaching a maximum absorption at the optimal organification degree of 2.62 wt% and then decreased. The enhancement of water absorbency is attributed to the fact that the introduction of OVMT into HEC-*g*-PAA could further improve its network structure in contrast to that doped with RVMT. The long alkyl chains of CTAB cations intercalated or absorbed between adjacent OVMT layers can form tiny hydrophobic region, by which the hydrogen bonding interaction among hydrophilic groups (−COOH, −OH and $-COO^-$) was weaken and intertwisting of polymer chains was prevented. So, the polymeric network can be regularly formed. Moreover, the spacing between the VMT layers was increased by intercalation of cationic long alkyl chains of CTAB, which facilitate a uniform dispersion of VMT platelets in the polymer matrix with an exfoliated structure and form nanocomposites. The better dispersion of OVMT also contributes to the improvement of polymeric network and increase of water absorbency [38]. Nevertheless, the water absorbency of HEC-*g*-PAA/OVMT decreased with further increasing organification degree of OVMT. The amount of hydrophobic alkyl chains in polymeric network increased as the organification degree increased, which means too many hydrophobic regions were formed and the hydro-

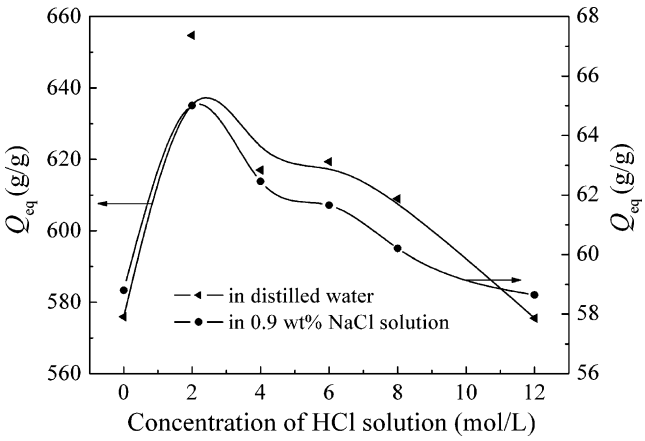

Fig. 5 Variation of water absorbency for the HEC-*g*-PAA/AVMT (10 wt%) superabsorbent nanocomposite with HCl concentration

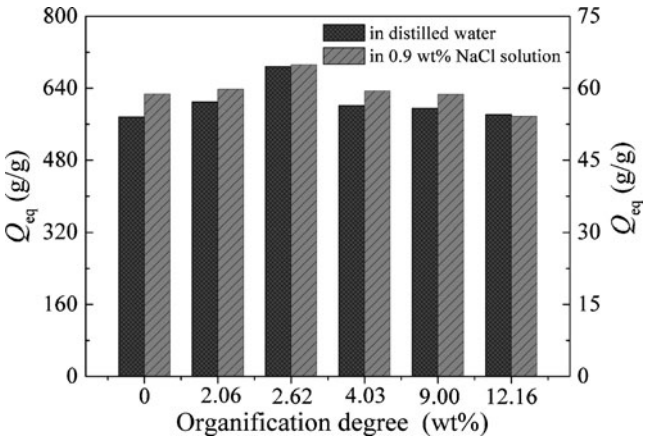

Fig. 6 Variation of water absorbency for the HEC-*g*-PAA/OVMT (10 wt%) superabsorbent nanocomposite with organification degree of OVMT

philicity of the HEC-*g*-PAA/OVMT nanocomposite decreases, leading to the shrinkage of water absorbency. Consequently, a suitable organification degree is needed for the HEC-*g*-PAA/OVMT nanocomposite to achieve the maximum water absorbency. This phenomenon is in conformity with our previous study on swelling behaviors of superabsorbent nanocomposite based on natural guar gum and organo-rectorite [38].

Swelling kinetics

When testing superabsorbent materials, swelling rate is another important evaluation index besides swelling capacity. The swelling kinetics of HEC-*g*-PAA/RVMT, HEC-*g*-PAA/AVMT and HEC-*g*-PAA/OVMT are shown in Fig. 7. It is found that the swelling rate of superabsorbents is fast during the initial 15 min, and then the swelling rate is slowed and swelling equilibrium can be achieved within 30 min. For the nanocomposites, the swelling kinetics can be evaluated by Schott's second-order swelling kinetic model (Eq. 7) [39]:

$$t/Q_t = 1/K_{is} + t/Q_{eq} \quad (7)$$

Q_t is the water absorbency at time t; $1/Q_{eq}$ is the inverse of maximum water absorbency; and $1/K_{is}$ is the reciprocal of the initial swelling rate. On the basis of the experimental data from Fig. 7, t/Q_t is plotted against time t to obtain better linear relationship, indicating that the second-order swelling kinetics is suitable to the evaluation of swelling process for the nanocomposites. From the slope and intercept of lines shown in Fig. 8, the values of the initial swelling rate (K_{is}) can be calculated and are listed in Table 1.

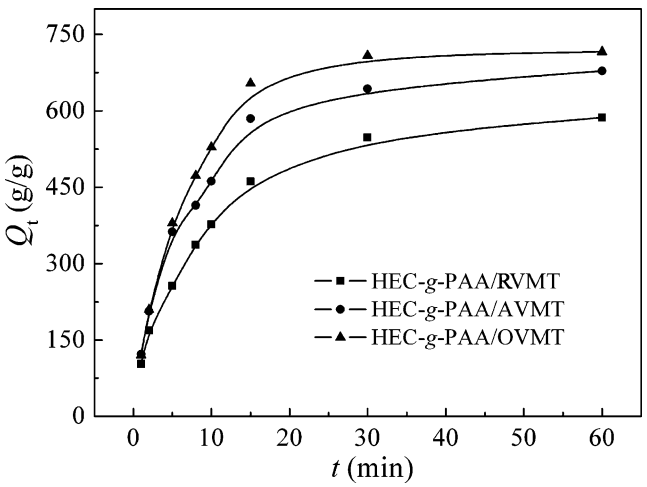

Fig. 7 Swelling kinetic curves of superabsorbents in distilled water. VMT content in the feed is 10 wt%

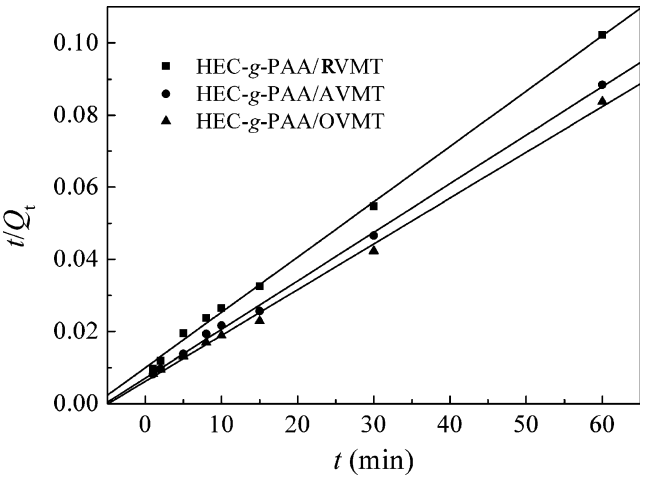

Fig. 8 t/Q_t versus t graphs of the superabsorbents in distilled water

As can be seen from Table 1, the initial swelling rate for each sample decreased in the order: HEC-*g*-PAA/OVMT > HEC-*g*-PAA/AVMT > HEC-*g*-PAA/RVMT. Both acid activation and organification modification of VMT improved the initial swelling rate of the superabsorbent. As mentioned above, the long alkyl chains of quaternary ammonium salt could weaken the hydrogen bond interaction among hydrophilic groups and improve the 3D network structure of the superabsorbent. This is favorable to the relaxation of polymer chains and the penetration of water molecules into the internal network, resulting in an enhancement of swelling rate. As for HEC-*g*-PAA/AVMT, appropriate acid activation of clay minerals can increase the amounts of exposed active Si–OH groups by disaggregation of clay particles and elimination of mineral impurities. According to previous research by Lee et al. [40], the initial swelling rate is primarily due to the penetration of water into the polymeric network through diffusion and capillarity. Therefore, the increased surface Si–OH groups after proper acid treatment of VMT will strengthen the affinity of the nanocomposite to water molecules and improve the initial swelling rate.

Table 1 Fitting results of the second-order swelling kinetics model

Samples	[a]K_{is}	[b]R
HEC-*g*-PAA/RVMT	100	0.999
HEC-*g*-PAA/AVMT	140	0.999
HEC-*g*-PAA/OVMT	161	0.998

[a] Initial swelling rate constant; (g_{water}/g_{gel})/min

[b] Linear correlation coefficient

Conclusions

The series of exfoliated superabsorbent nanocomposites based on HEC, raw VMT, acidified VMT and organo-VMT were prepared by free-radical solution polymerization. FTIR, XRD and TEM results indicate that the −OH groups of HEC and VMT participated in the graft polymerization with AA, and the layer VMT clay was exfoliated and formed a nanocomposite structure. The incorporation of VMT greatly enhanced the water absorbency of superabsorbent, and the water absorbency of the nanocomposite incorporating 40 wt% of VMT is still as much as that of VMT-free sample, which is favorable to reduce the production cost. The facile modification of RVMT by acidification and organification can improve the water absorbency to a high degree than raw one. The swelling rate was obviously improved due to the acidification and organification modification of RVMT, the nanocomposite derived from OVMT gives the best swelling capability and swelling rate in contrast to that from raw or acidified VMT. Thus, the utilization of biodegradable HEC and inexpensive VMT clay minerals effectively reduced production cost and render the superabsorbent eco-friendly, and more excellent properties can be achieved by facilely a facile acidification and organification of VMT.

Acknowledgement This work was financially supported by the West Light Foundation and the Western Action Project of CAS (No. KGCX2-YW-501) and "863" Project of the Ministry of Science and Technology, P. R. China (No. 2006AA03Z0454 and 2006AA100215).

References

1. Kosemund K, Schlatter H, Ochsenhirt JL, Krause EL, Marsman DS, Erasala GN (2009) Regul Toxicol Pharm 53:81–89
2. Sadeghi M, Hosseinzadeh HJ (2008) J Bioact Compat Pol 23:381–404
3. Dzinomwa GPT, Wood CJ, Hill DJT (1997) Polym Adv Technol 8:767–772
4. Teodorescu M, Lungu A, Stanescu PO, Neamtu C (2009) Ind Eng Chem Res 48:6527–6534
5. Liu MZ, Liang R, Zhan FL, Liu Z, Niu AZ (2006) Polym Adv Technol 17:430–438
6. Zhao GZ, Liu YQ, Tian Y, Sun YY, Cao Y (2009) J Polym Res 17:119–125
7. Kaşgöz H, Durmus A (2008) Polym Adv Technol 19:838–845
8. Dhodapkar R, Rao NN, Pande SP, Nandy T, Devotta S (2007) React Funct Polym 67:540–548
9. Pourjavadi A, Barzegar S, Mahdavinia GR (2006) Carbohydr Polym 66:386–395
10. Ray SS, Bousmina M (2005) Prog Mater Sci 50:962–1079
11. Al E, Güçlü G, Yim TB, Emik S, Özgümü S (2008) J Appl Polym Sci 109:16–22
12. Kiatkamjornwong S, Chomsaksakul W, Sonsuk M (2000) Radiat Phys Chem 59:413–427
13. Demitri C, Sole RD, Scalera F, Sannino A, Vasapollo G, Maffezzoli A, Ambrosio L, Nicolais L (2008) J Appl Polym Sci 110:2453–2460
14. Pourjavadi A, Ghasemzadeh H, Mojahedi F (2009) J Appl Polym Sci 113:3442–3449
15. Hua SB, Wang AQ (2009) Carbohydr Polym 75:79–84
16. Xie YT, Wang AQ (2009) J Polym Res 16:143–150
17. Zhang JP, Wang Q, Wang AQ (2007) Carbohydr Polym 68:367–374
18. Wang WB, Zheng YA, Wang AQ (2008) Polym Adv Technol 19:1852–1859
19. Abd El-Mohdy HL, Abd El-Rehim HA (2009) J Polym Res 16:63–72
20. Pourjavadi A, Hosseinzadeh H, Sadeghi M (2007) J Compos Mater 41:2057–2069
21. Mohamadnia Z, Zohuriaan-Mehr MJ, Kabiri K, Razavi-Nouri M (2008) J Polym Res 15:173–180
22. Sannino A, Demitri C, Madaghiele M (2009) Materials 2:353–373
23. Wang AQ, Zhang JP (2006) Organic/inorganic superabsorbent composites (Chinese). Science, Beijing
24. Lee WF, Chen YC (2005) J Appl Polym Sci 97:855–861
25. Xu J, Meng YZ, Li RKY, Xu Y, Rajulu AV (2003) J Polym Sci Part B: Polym Phys 41:749–755
26. Zheng Y, Li P, Zhang JP, Wang AQ (2007) Eur Polym J 43:1691–1698
27. Zhao DF, Zhou J, Liu N (2006) Appl Clay Sci 33:161–170
28. de Paiva LB, Morales AR, Díaz FRV (2008) Appl Clay Sci 42:8–24
29. Li X, Xu SM, Wang JD, Chen XZ, Feng S (2009) Carbohydr Polym 75:688–693
30. Flory PJ (1953) Principles of polymer chemistry. Cornell University Press, NewYork
31. Li A, Wang AQ, Chen JM (2004) J Appl Polym Sci 92:1596–1603
32. Liu DF, Du XS, Meng YZ (2006) Mater Lett 60:1847–1850
33. Post JE, Heaney PJ (2008) Am Mineralogist 93:667–675
34. Utracki LA, Sepehr M, Boccaleri E (2007) Polym Adv Technol 18:1–37
35. Galan E (1996) Clay Miner 31:443–453
36. Zhang KY, Hu HP, Zhang LJ, Chen QY (2008) T Nonferr Metal Soc 18:1285–1289
37. Lee WF, Yang LG (2004) J Appl Polym Sci 92:3422–3429
38. Wang WB, Wang AQ (2009) Carbohydr Polym 77:891–897
39. Schott H (1992) J Macromol Sci B 31:1–9
40. Lee WF, Wu RJ (1996) J Appl Polym Sci 62:1099–1114